Local Analysis of Confidence Measures for Optical Flow Quality Evaluation

Patricia Márquez-Valle[1], Debora Gil[1], Rudolf Mester[2] and Aura Hernàndez-Sabaté[1]

[1]*Computer Vision Center, Universitat Autònoma de Barcelona, Edifici O - Campus UAB, Bellaterra, Barcelona, Spain*
[2]*Visual Sensorics and Information Processing Lab, J. W. Goethe Universität, Frankfurt, Germany*

Keywords: Optical Flow, Confidence Measure, Performance Evaluation.

Abstract: Optical Flow (OF) techniques facing the complexity of real sequences have been developed in the last years. Even using the most appropriate technique for our specific problem, at some points the output flow might fail to achieve the minimum error required for the system. Confidence measures computed from either input data or OF output should discard those points where OF is not accurate enough for its further use. It follows that evaluating the capabilities of a confidence measure for bounding OF error is as important as the definition itself. In this paper we analyze different confidence measures and point out their advantages and limitations for their use in real world settings. We also explore the agreement with current tools for their evaluation of confidence measures performance.

1 INTRODUCTION

Optical flow is a powerful tool for 3D reconstructions, pedestrian detection, surveillance systems, medical imaging assessment, etc. Its computation in real-world is a challenging task due to, among others, illumination changes, noise or textureless regions (Barron et al., 1994). Most of current research focus their efforts on defining new algorithms in order to reduce the impact of OF inaccuracies produced by the above artifacts. Current algorithms are tested and compared to each other by means of databases with ground truth (McCane et al., 2001; Baker et al., 2011; Liu et al., 2008; Butler et al., 2012). However, most of the available scenarios of databases are poorly assorted (urban, small objects, etc.) with only changes on illumination and object motion. Another concern is that the number of frames available for each sequence may be small. Even though recent databases for optical flow evaluation are more realistic, they are far from modeling the complexity and variability of real sequences (Butler et al., 2012). Consequently, even if a method performs properly on such databases, its performance could fail in real-world conditions.

In order to use optical flow in a confident decision support system, a mechanism to detect sequence pixels that have high error in their computations is of prime importance. In this context, Confidence Measures (CM) should be an indicator of the accuracy of the output of an optical flow algorithm. It should be noted that a confidence measure can provide at most an upper bound of OF error at each pixel, not its real value (according to numerical error analysis (Cheney and Kincaid, 2008)). This implies that high values of the confidence measure should ensure a low OF error, while for low CM values errors could take any value. Points that have high error and high value of the confidence measure are unpredictable points which CM can not discard and, thus, should be the least possible.

Evaluating the quality of a confidence measure, as well as analyzing the origin of unpredictable points, are issues as important as the definition of a confidence measure itself. Up to our knowledge, the only ways of assessing CM performance are the Sparsification Plots, SP, introduced in (Bruhn and Weickert, 2006) and Error Prediction Plots, EPP, introduced in (Márquez-Valle et al., 2012). On the one hand, SP show the average OF error across CM percentiles. Sparsification plot is the most widespread tool for studying the general behavior of confidence measures allowing an overall comparison across measures. However, being based on error global statistics, they are not well suited for detecting unpredictable points. On the other hand, EPP partially overcome such limitation and, by definition, they are better designed to detect artifacts in CM-OF error scatter plots. A main concern is that, none of the existing CM eval-

uations explore the local pixel-wise behavior of confidence measures and the sources of unpredictable points.

In this paper we propose exploring the sources of unpredictable points for existing types of CM. We present two main contributions. First, we analyze the local image intensity and OF patterns in order to determine the sources of CM failing cases. Second, we explore whether CM error bounding capabilities are reflected by current ways of evaluating CM performance. In this manner, this paper settles the ground for further improvement of confidence measures and their evaluation.

The paper is organized as follows. Section 2 briefly describes the state of the art confidence measures and performance evaluation methods. Section 3 analyzes, through some examples, the capabilities of confidence measures for bounding the error. There is also an analysis of the capabilities of SP and EPP to detect when the confidence measures are able to bound the error. Finally, the discussions, conclusions and future work are given in section 4.

2   STATE OF THE ART

This section is devoted to briefly describe how most of optical flow techniques compute the flow field, and also identify the different types of errors they can produce. As well, in this section, the state of the art confidence measures and current frameworks that allow to evaluate CM's performance are described.

Most of current optical flow techniques compute the flow field by minimizing a variational (Horn and Schunck, 1981) that combines a data-term and a smoothness-term:

$$E(u,v) = \int \underbrace{D(u,v,\nabla I)}_{\text{Data Term}} + \alpha \underbrace{S(\nabla u, \nabla v)}_{\text{Smoothness Term}} \, dx \, dy \quad (1)$$

for $I(x,y,t)$ denoting the image sequence, (u,v) the flow field and ∇ the sequence gradient. The data-term is usually based on the optical flow constraint, $I_x u + I_y v + I_t = 0$, and the smoothness-term models the general properties of the flow field. The minimum of (1) is computed by solving the associated Euler-Lagrange equations.

Errors of the resulting flow can be split into two main categories (Márquez-Valle et al., 2012): errors in OF model and numerical errors:

Model Errors. The formulation of optical flow relies on some assumptions on the input data and flow motion. Brightness constancy constraint, or some regularity of the motion flow (Horn and Schunck, 1981;

Lucas and Kanade, 1981) are common assumptions of optical flow algorithms. In case these assumptions are not satisfied (brightness changes for instance) the output vector is less reliable and might fail to properly model sequence motion.

Numerical Errors. The input data for OF computation might contain errors that are propagated through the computations, and, thus, introduce errors in the output flow. The impact of input errors propagation, depends on the numerical stability of optical flow formulation and can be explored by means of numeric analysis tools (Cheney and Kincaid, 2008).

2.1   Confidence Measures

The final purpose of a confidence measure should be the detection of numerical errors and also, provide an upper bound for the final error. Even though in the literature there are several different confidence measures defined (Singh, 1990; Barron et al., 1994; Shi and Tomasi, 1994; Bruhn and Weickert, 2006; Kondermann et al., 2008; Sundaram et al., 2010; Kybic and Nieuwenhuis, 2011; Gehrig and Scharwachter, 2011; Márquez-Valle et al., 2012; Mac Aodha et al., 2013; Senst et al., 2012), we only explore four of the most representative ones:

Energy. Under the (sensible) assumption that all constrains have been taken into account in the definition of the functional (1), the computed flow field will be accurate in the measure that its local energy is low. Under this consideration, the authors in (Bruhn and Weickert, 2006) propose the following measure:

$$c_e = \frac{1}{D(u,v,\nabla I) + \alpha S(\nabla u, \nabla v) + \varepsilon^2} \quad (2)$$

where ε prevents dividing by zero. A main advantage of c_e is that it can be computed for any variational scheme. A main concern is that c_e only measures that (u,v) minimizes equation (1) and, thus, fulfills the assumptions made in the model. However, this does not guarantee that (u,v) corresponds to the true flow field, since defining the most appropriate optical flow constraints for a given application is still an open problem.

Statistical. In many applications, flow fields follow similar local motion patterns. If such motion patterns are learned a priori, then a classifier can be used to define a confidence measure. The measure introduced in (Kondermann et al., 2008), which we note as c_s, derives natural motion statistics from sample data and carries out a hypothesis test to obtain confidence values for the computed flow. The method depends only

on the resulting flow field and on the prior knowledge learned from a database. The confidence measure assesses the computed optical flow calculating the local variability by means of the Mahalanobis distance between the computed vector and the distribution given by the surrounding ones. Since the formulation is not straight forward, we refer the reader to the paper (Kondermann et al., 2008) for more details.

A main limitation of this measure is that unusual motion patterns are not easy to learn and might require a huge database of different flow patterns to train the model. This limits its use for sequences with flow fields that are erratic or unpredictable. In addition, it only assesses if the flow field is coherent, but not if the flow field corresponds to the sequence motion.

Bootstrap. The measure introduced in (Kybic and Nieuwenhuis, 2011) aims at assessing the uncertainty of the optical flow method with respect to the model constraints. That is, they compute the variability of the computed flow field using bootstrap by introducing numerical perturbations. If the variability is high, the flow field is not reliable, whereas for low variability, the computation is reliable. In order to have a decreasing dependency with the accuracy is rewritten follows:

$$c_b = \frac{1}{\psi_{bootg} + \varepsilon^2}, \quad \psi_{bootg} = \sqrt{\sigma_u^2 + \sigma_v^2} \quad (3)$$

where ε prevents dividing by zero, and σ_u and σ_v are the variances of the flow field (u, v) after the boostrap computation. For more details of ψ_{bootg} defined in (Kybic and Nieuwenhuis, 2011), we refer the reader to eq. (15) of that paper. Like c_e, this one also assesses the consistency of the model assumptions, but also assesses the errors produced by numerical stability of the method. However, c_b requires to be redefined for each optical flow technique and it is computationally costly.

Image Local Structure. Some confidence measures are defined by means of the structure tensor of the image, and thus, they use information about the local structure of the image. There are several measures derived from the structure tensor: determinant, trace (Barron et al., 1994), lowest eigenvalue (Shi and Tomasi, 1994) among others. These measures only detect errors produced due to the image, that is, textureless regions, noise, etc. However, they do not consider the errors produced by during the computations. An improved measure that uses the structure tensor, considers the condition number of the structure tensor matrix (Márquez-Valle et al., 2012):

$$c_K = \frac{\lambda_{min}}{\lambda_{max}} \quad (4)$$

for λ_{min} and λmax the minimum and maximum eigenvalues of the structure tensor at a given pixel location. This measure, not only assesses the capabilities of the image to compute the flow field, but also assesses the numerical stability of the computation for Lucas-Kanade based schemes (Lucas and Kanade, 1981; Bruhn et al., 2005).

2.2 Performance Evaluation of Confidence Measures

Scatter plots showing CM against OF errors are a good tool to assess the relation between both quantities, as illustrated in fig.1. A perfect CM should produce decreasing profiles, like the one shown in middle plots. Points inside the red square in the first scatter correspond to points which error is not bounded by the confidence measure. Given that those points could introduce a significant error in a decision support system using OF, evaluation of the confidence measure should detect the scope of such unpredictable points.

The most extended way to represent the performance of a confidence measure is by means of the Sparsification Plots, SP (Bruhn and Weickert, 2006). Such plots are given by the remaining mean error for fractions of removed flow vector having increasing confidence measure values. That is, the confidence measure is increasingly sorted, then, from 0% to 100%, a percentage of flow vectors is removed and the average error of the remaining ones is computed. The arrows of the scatter plots shown in the first row of fig.1 illustrate the computation of the SP shown in the last plot. Under the assumption that higher values of the confidence measure are associated to lower optical flow errors, the sparsification plots should have decreasing profiles. An increase in their values for the higher removed fractions indicates artifacts in the decreasing dependency possibly due to a high error. However, the inverse does not always hold and random uniform dependencies could produce sensible plots. This is the case of the first representative sequence shown in fig. 1. Even if the dependency shown in the scatter plot is worse in the first sequence, its SP (blue line in the last plot of fig1) indicates a better performance for higher fractions.

Another way to represent the performance of confidence measures are the Error Prediction Plots, EPP (Márquez-Valle et al., 2012). Such plots provide a global vision of the capability of confidence measures to discard high errors. The error prediction plots are computed by means of the conditional probabilities across the diagonal of the CM-OF error scatter plots.

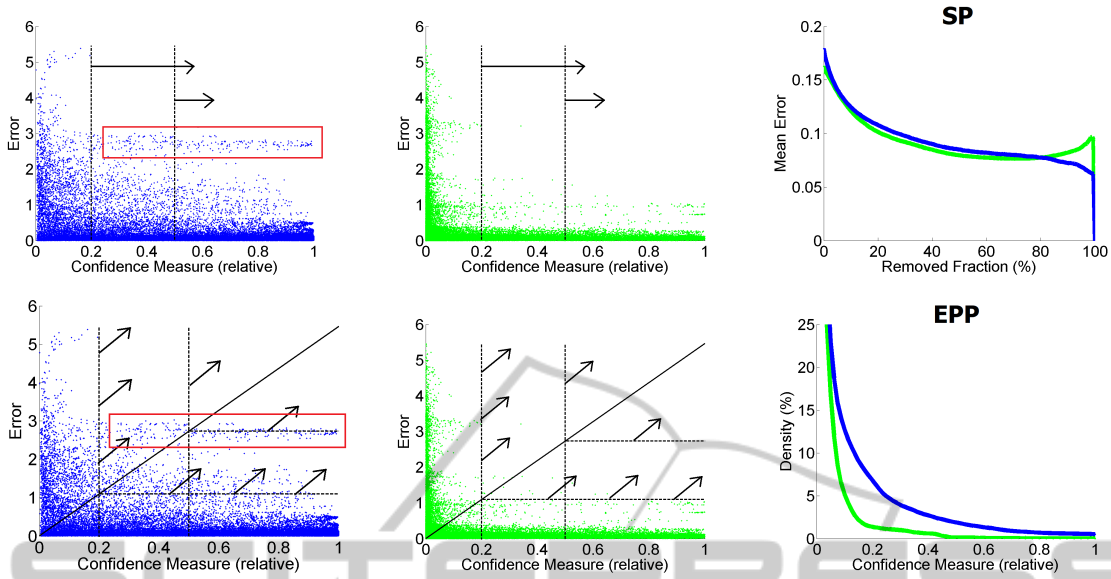$$P_C(\tau_{EE}, \tau_{CM}) := P(EE \geq \tau_{EE} | CM \geq \tau_{CM}) \quad (5)$$

Figure 1: Existing evaluations of Confidence Measures: first row, SP and second row, EPP. First and second columns show Scatter plots of a confidence measure versus OF errors (for two different cases colored in blue and green). Red squares on the first column denote outliers. The black lines and arrows show how the SP and EPP are computed respectively. SP and EPP of both measures are shown on third column.

for $P_C(\tau_{EE}, \tau_{CM})$ the probability of having an error EE above τ_{EE} provided that CM is above τ_{CM}. Taking into account that the condition $CM \geq \tau_c$ corresponds to a vertical line and $EE \geq \tau_{EE}$ to an horizontal one, the conditional probability is given by the fraction of points lying on the superior quadrant defined by the former lines. The EPP are defined as the plot given by $(CM, P_C(EE_{max} \cdot CM/CM_{max}, CM))$, for EE_{max} the maximum error allowed by the application and CM_{max}, CM maximum value. The scatter plots in the second row of fig.1 illustrate the computation of (5) for two representative cases. Arrows indicate the points that are considered for the computation of conditional probabilities. Unlike the SP shown in the first row of fig.1, we observe that EPP is worse for the non-decreasing case.

3 ANALYSIS OF CONFIDENCE MEASURES

The main purpose of this section is to help to better understand a confidence measure behavior and its weak and strong points for bounding OF error. In particular we will address two main issues: first, we are interested in finding the local conditions (both in appearance and motion) that a sequence should fulfill in order that a CM succeeds in bounding the error of a particular OF method. Second, we will assess, the capability of SP and EPP for detecting those points

where the confidence measure is not able to bound the error.

In order to explore CM bounding capabilities we locally analyze the behavior of confidence measures for a selected sample of sequence patches. These patches cover the main appearance and motion features that are prone to introduce an error in OF and CM expected behaviors. In this context we have selected patches violating:

- **Data-term OF Constrain Assumptions.** On the one hand, the data term requires that there is enough information in the image intensity to compute the apparent 2D motion. On the other hand, large displacements are against the first order Taylor approximation given by the OF equation. Therefore, we have selected patches with straight edges and textureless regions for their intensity appearance as well as, patches of a large displacement.

- **Smoothness-term Regularity Assumptions.** Independent motions might interfere with the regularity assumptions of the smoothness-term.

The maximum error used to compute EPP is $EE_{max} = 2$. We have considered the 4 confidence measures described in section 2, c_k, c_e, c_b and c_s. Results have been extracted from the Middlebury database (Baker et al., 2011). This database contains real-life and synthetic sequences with ground truth, to show some examples we have used two frames of the RubberWhale and the Urban sequences. Motion

has been computed using the Combined Local-Global (CLG) scheme (Bruhn et al., 2005) as implemented in (Liu, 2009) [1]. The error score is the End-Point Error (*EE*) (Baker et al., 2011), it measures the difference between computed flow field and ground truth.

Figures 2 and 3 show our analysis for Rubber-Whale and Urban3 sequences. Each figure shows a sequence frame, four representative patches with computed (yellow arrows) and ground truth (green arrows) flows, CM-OF error scatter plots for each measure and SP, EPP plots. Each patch is of size 7×7 and it is centered at the respective illustrative point shown in the sequence frame and scatter plots.

Patches in fig.2 contain straight edges with independent motions (patches 1 and 4), a textureless region with uniform motion (patch 2), and a textureless region with a slightly irregular motion (patch 3). Patches in fig. 3 show a sloped border with a large displacement of an object moving over a static background (patch 1), textureless regions with uniform motions (patches 2 a 4) and a slightly textured region with uniform motion (patch 3).

Concerning data term conditions, at straight edges (patches 1, 4 in fig.2) and textureless regions (patch 2, 3 in fig.2 and 2,4 in fig.3) CLG can not solve the data term. The lowest eigenvalue of the structure tensor matrix is close to zero and this introduces large numerical instability. We would like to note that in such cases EE can take any value, ranging within 0 and 20 in our sequences. Numerical instability of the data term is properly detected by low c_k values. The data term is numerically well-conditioned in the case of sloped borders (patch 1 in fig.3) and textured regions (patches 3 in fig.2 and 3). However, stable numerics do not guarantee accurate OF, given that OF model assumptions are also decisive for its accuracy. This is the case of patch 1 in fig.3, which presents a high error due to the high displacement magnitude and, thus, c_k can not properly bound EE.

Regarding regularity conditions, the bounding capabilities of c_b are more related to them assumptions and, thus, it properly bounds EE at patches presenting independent moving objects (like patches 1, 4 in fig.2 and patch 1 in fig.3). However, its capabilities for error bounding decrease for patches with uniform motion, given that c_b is always high, but OF might present a large error for textureless patches (patch 2 in fig.2). The measure based on energy minimization, c_e, is also associated to model assumptions, given that at pixels which model regularity is not met, the functional can not be properly minimized. This is the case of patches with independent motions, like patches 1, 3, 4 in fig.2 and patch 1 in fig.3. Like c_b, c_e fails in

---
[1] Available at http://people.csail.mit.edu/celiu/OpticalFlow/

the case of textureless regions with uniform motion shown in patch 2 in fig.2 and patch 3 in fig.3.

Finally, the weakest measure for error bounding purposes is c_s, which scatters present the most uniform distribution of all. Such uniform distribution of EE across c_s values indicates that there is not a clear relation between the measure and the error. In fact, it only succeeds in bounding EE for patch 3 in fig.2 and patch 1 in fig.3 that are the ones having a flow field not regular around the central point. For the remaining patches, OF is regular enough although this does not necessarily imply it is accurate.

Concerning CM performance evaluation shown in bottom plots, we note that the bounding artifacts detected in c_e profile in fig.2 are not properly reflected by SP plots. On the contrary, c_k decreasing profiles do not always produce a best decreasing SP (fig.2). This is due to only considering 1-dimensional statistics over *EE* and not over the bimodal distribution given by (CM, EE). By considering bimodal statistics, *EPP* provides a better ordering of *CM* quality for error bounding. In particular, it detects the groups of unpredictable pixels introducing horizontal scatters in *CM-EE* plots, like the ones present in c_b and c_e scatter plots in fig.3.

4 DISCUSSIONS, CONCLUSIONS AND FUTURE WORK

Evaluating the capabilities of a confidence measure for optical flow error bounding is as important as its definition. In this paper we have analyzed locally the capabilities of confidence measures for bounding the different types of OF error. We have also evaluated if current tools for confidence measure quality assessment agree with confidence measures bounding capabilities. Concerning the capabilities of existing CMs for OF error bounding, the following interesting points are derived from our analysis:

Energy (c_e) confidence measure detects when the functional is not properly minimized, and this usually happens at borders. In addition, this confidence measure only detects points where the computation does not correspond with the model assumptions, and thus it detects points that satisfy the model assumptions as reliable although they may not coincide with the ground truth.
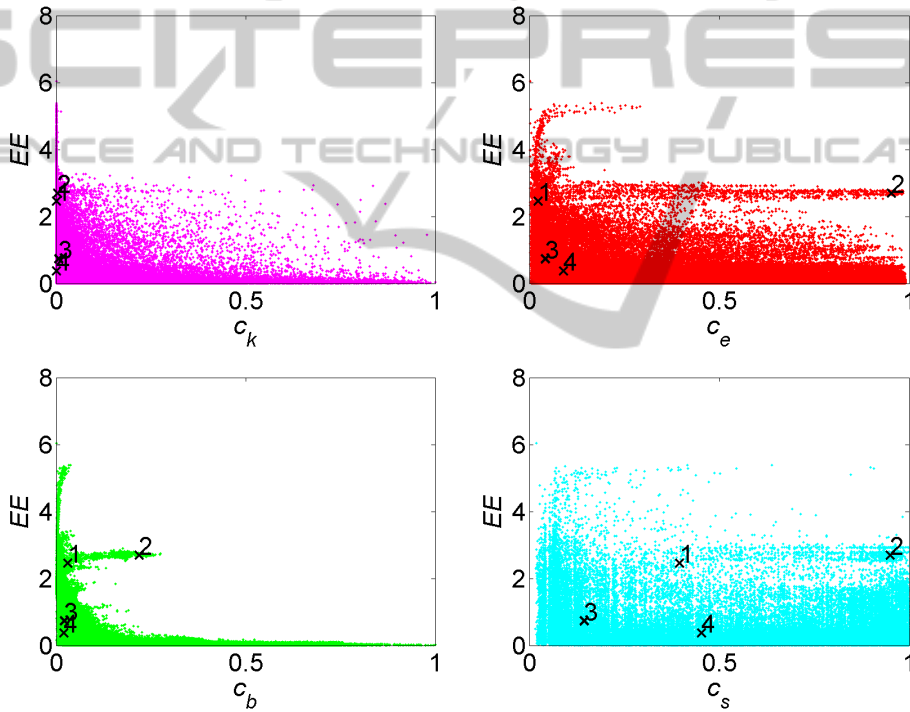
Statistical (c_s) confidence measure detects if the computed flow is not coherent, and, thus, points having an OF either not regular or random. This implies that a constant OF would always be reliable regardless of its agreement with ground truth.

Illustrative Points
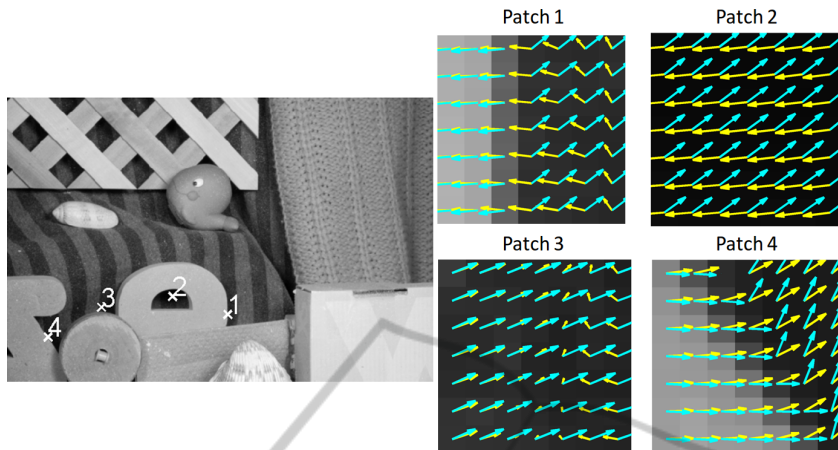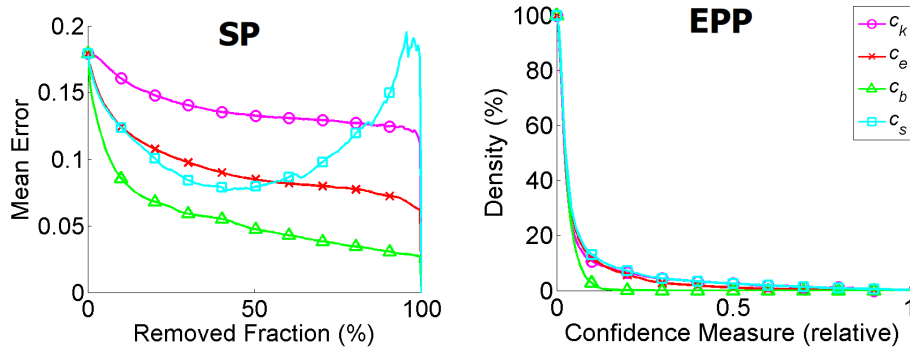

Scatter Plots

Performance Evaluation

Figure 2: RubberWhale sequence.

Illustrative Points

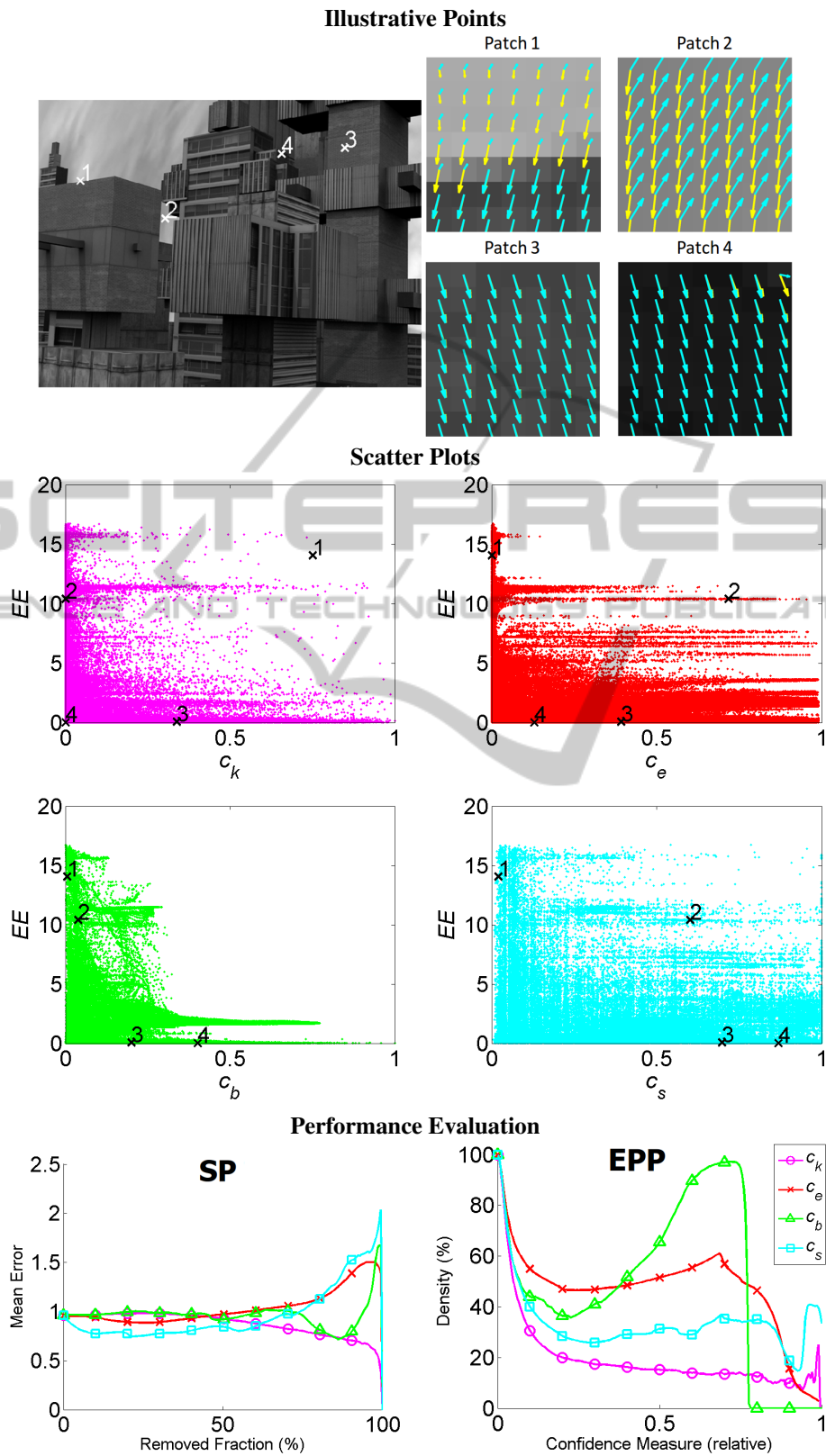**Scatter Plots**

Performance Evaluation

Figure 3: Urban3 sequence.

Bootstrap (c_b) confidence measure detects if the model is unstable, that is, when small perturbations in the input data produce high variations in the output. Thus, it detects points that do not satisfy model assumptions like edges of object following different motions and textureless regions.

Image Local Structure (c_k) confidence measure detects those pixels the image structure is not appropriate to solve optical flow, like textureless regions, and straight lines. However, textured regions may contain a lot of noise disturbing computations and, also, failing of OF assumptions is not considered.

We conclude that c_s is not the best suited for bounding OF error. Besides, c_k, c_b, c_e are able to bound a different kinds of error and, in fact, they provide complementary bounds.

Concerning existing methods for evaluation of confidence measures, EPP better reflect non-decreasing profiles between CM and OF error and, thus, it is better suited for detecting CM unable to bound errors for a significant amount of cases. However, none of the evaluation methods provides enough information about confidence measures failing cases and thus, further research is required.

As a future work it would be interesting to view examples for patches with more than two motion areas and illumination changes. Also use a larger database. And finally, check the confidence measure performances on different optical flow methods.

ACKNOWLEDGEMENTS

REFERENCES

Baker, S., Scharstein, D., Lewis, J., and et al. (2011). A database and evaluation methodology for optical flow. *IJCV*, 92(1):1–31.

Barron, J. L., Fleet, D. J., and Beauchemin, S. S. (1994). Performance of optical flow techniques. *IJCV*, 12(1):43–77.

Bruhn, A. and Weickert, J. (2006). A confidence measure for variational optic flow methods. In *Geometric Properties for Incomplete Data*, pages 283–298.

Bruhn, A., Weickert, J., and Schnörr, C. (2005). Lucas/Kanade meets Horn/Schunck: Combining local and global opticflow methods. *IJCV*, 61(2):221–231.

Butler, D. J., Wulff, J., Stanley, G. B., and Black, M. J. (2012). A naturalistic open source movie for optical flow evaluation. In *ECCV*, pages 611–625.

Cheney, W. and Kincaid, D. (2008). *Numerical Mathematics and Computing, Sixth edition*. Bob Pirtle, USA.

Gehrig, S. and Scharwachter, T. (2011). A real-time multi-cue framework for determining optical flow confidence. In *ICCV Workshops*, pages 1978–1985. IEEE.

Horn, B. and Schunck, B. (1981). Determining optical flow. *AI*, 17:185–203.

Kondermann, C., Mester, R., and Garbe, C. S. (2008). A statistical confidence measure for optical flows. In *ECCV*, pages 290–301.

Kybic, J. and Nieuwenhuis, C. (2011). Bootstrap optical flow confidence and uncertainty measure. *Computer Vision and Image Understanding*, pages 1449–1462.

Liu, C. (2009). *Beyond pixels: exploring new representations and applications for motionanalysis*. PhD thesis, Cambridge, MA, USA.

Liu, C., Freeman, W., Adelson, E., and Weiss, Y. (2008). Human-assisted motion annotation. In *CVPR*.

Lucas, B. and Kanade, T. (1981). An iterative image registration technique with an application to stereovision. In *DARPA IU Workshop*, pages 121–130.

Mac Aodha, O., Humayun, A., Pollefeys, M., and Brostow, G. J. (2013). Learning a confidence measure for optical flow. *IEEE Trans. Pattern Anal. Mach. Intell.*, 35(5):1107–1120.

Márquez-Valle, P., Gil, D., and Hernàndez-Sabaté, A. (2012). A complete confidence framework for optical flow. In *ECCV Workshops*, volume 7584 of *LNCS*, pages 124–133. Springer.

McCane, B., Novins, K., Crannitch, D., and Galvin, B. (2001). On Benchmarking Optical Flow. *Computer Vision and Image Understanding*, 84(1).

Senst, T., Eiselein, V., and Sikora, T. (2012). Robust local optical flow for feature tracking. *IEEE Trans. Circuits Syst. Video Techn.*, 22(9):1377–1387.

Shi, J. and Tomasi, C. (1994). Good features to track. In *CVPR*, pages 593–600.

Singh, A. (1990). An estimation-theoretic framework for discontinuous flow fields. In *ICCV*, pages 168–177.

Sundaram, N., Brox, T., and Keutzer, K. (2010). Dense point trajectories by gpu-accelerated large displacement optical flow. In *ECCV*, pages 438–451.